Eco-Friendly Synthesis of Iron Oxide Nanoparticles Using Plants: Structural Insights and Biological Significance

Nikita., Ashu Chaudhary*

Department of Chemistry, Kurukshetra University, Kurukshetra-136119, Haryana, India

***Corresponding Author**

DOI: https://doi.org/10.51584/IJRIAS.2026.11060167

Received: 29 May 2026; Accepted: 03 June 2026; Published: 06 July 2026

ABSTRACT

Iron oxide nanoparticles (FeONPs) have emerged as an important class of nanomaterials owing to their remarkable magnetic, physicochemical, catalytic, and biocompatible properties. Various forms of iron oxides, including hematite, magnetite, maghemite, ferrihydrite, and wüstite, exhibit distinct crystal structures, space groups, lattice parameters, morphologies, and functional characteristics that significantly influence their properties and applications. Although several physicochemical methods have been developed for the synthesis of FeONPs, these approaches often involve toxic chemicals, high energy consumption, and harsh reaction conditions. Consequently, plant-mediated green synthesis has attracted considerable attention as a sustainable and eco-friendly alternative, where phytochemicals serve as natural reducing and stabilizing agents during nanoparticle formation. Compared with conventional methods, green synthesis offers several advantages, including low toxicity, cost-effectiveness, environmental compatibility, and suitability for large-scale production. Owing to their multifunctional nature, green synthesized FeONPs have shown promising potential in antimicrobial, anticancer, and many other biological applications. This review highlights the different forms of iron oxide nanoparticles, their structural and physicochemical characteristics, plant-mediated green synthesis strategies, and emerging biological applications.

Keywords: Iron nanoparticles, Green synthesis, Anticancer activity, Antioxidant activity

Graphical Abstract:

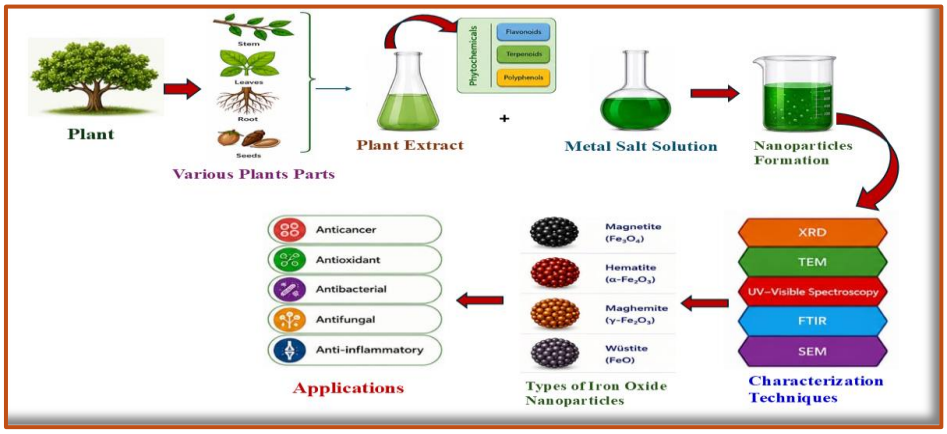

INTRODUCTION

In recent decades, nanotechnology has emerged as one of the most transformative and rapidly advancing fields of science, offering innovative solutions to several global challenges related to healthcare, environmental sustainability, energy, and industrial development. The extraordinary properties exhibited by nanomaterials at the nanoscale have attracted immense attention from researchers worldwide. Among these nanomaterials, nanoparticles (NPs), typically ranging from 1 to 100 nm in size, have gained significant importance due to their unique physicochemical characteristics, including high surface area, enhanced catalytic activity, and

ISSN No. 2454-6194 | DOI: 10.51584/IJRIAS |Volume XI Issue VI June 2026

remarkable optical properties [1]. These distinctive features have enabled nanoparticles to play a crucial role in diverse fields such as agriculture [2], medicine [3], electronics [4], chemistry [5], and pharmaceuticals [6].

Among the different classes of nanoparticles, iron-based nanoparticles (FeNPs) including hematite (α-Fe_2O_3), magnetite (Fe_3O_4), maghemite (γ-Fe_2O_3), and various mixed ferrites have attracted significant interest due to their remarkable magnetic, catalytic, and biocompatible characteristics. These nanoparticles have been widely explored for diverse applications such as environmental remediation, magnetic resonance imaging (MRI), targeted drug delivery, biosensing, and cancer hyperthermia therapy [7]. To achieve such diverse functional properties and application-specific performance, the development of efficient synthesis approaches with precise control over nanoparticle morphology and size has become essential. Various synthetic strategies have been developed to fabricate nanoparticles with controlled morphology and size. Generally, two fundamental routes are adopted for nanoparticle synthesis-the top-down and bottom-up techniques. In the top-down strategy, bulk materials are reduced to the nanoscale using physical techniques such as ball milling, laser ablation, lithography, etching, spark ablation, chemical vapor deposition (CVD), and ultrasonic spray pyrolysis. In contrast, in the bottom-up approach, nanoparticles are formed by assembling atomic or molecular precursors using chemical or physicochemical techniques, including chemical reduction, sol–gel synthesis, hydrothermal and solvothermal techniques, CVD, microwave-assisted synthesis, and electrochemical deposition [8]. These synthesis methods for nanoparticles are often resource- and energy-intensive, involving toxic chemicals and harsh reaction conditions. Such practices not only increase production costs and processing time but also generate hazardous by-products, posing significant risks to environmental sustainability and biological systems. Consequently, green synthesis presents several advantages over conventional methods, as it is cost-effective, environmentally sustainable, and readily adaptable for large-scale production. This approach avoids the utilization of toxic chemicals, extreme temperatures, and high energy requiring procedures. Additionally, green synthesis provides improved control and reproducibility in nanoparticle crystallization. Nanoparticles produced through green methods are economically viable and possess diverse applications across scientific fields [9]. The green synthesis of metal and metal oxide nanoparticles has utilized various biological sources, including plant extracts, bacteria, and algae. Among the green synthesis strategies, plant-mediated synthesis is particularly advantageous, offering a rapid, straightforward, and scalable approach for large-scale nanoparticle production, in contrast to methods relying on algae, fungi, or bacteria [10]. Plants are extensively employed in nanoparticle synthesis due to their abundance of phytochemicals, which act as natural reducing and stabilizing agents throughout the nanoparticle formation process. Compounds such as flavonoids [11], terpenoids, amines, phenol [12] and carbohydrates [13] facilitate the synthesis and growth of FeO nanoparticles. These biomolecules provide diverse chemical functional groups that contribute to the reduction, oxidation, and stabilization of metal oxide precursors [14]. The differences in phytochemical composition among plants influence their capacity to reduce metal ions, thereby impacting nanoparticle yield. Plant extracts promote both the reduction and stabilization of metal ions, resulting in a uniform particle size distribution. Flavonoids, as secondary metabolites, possess oxygen-scavenging properties that enhance their electron-donating capacity. Similarly, phenolic compounds, including protocatechuic acid, caffeic acid, and gallic acid, contain hydroxyl groups capable of interacting with metal ions. The reduction potential of these polyphenolic compounds is adequate to convert metallic iron into zero-valent iron, leading to the formation of magnetic $FeONP_S$ [15]. In the past decade, nanoparticle synthesis, particularly the green synthesis of iron nanoparticles, has received considerable prominence due to their safer profile compared to other metallic nanoparticles. Bio fabricated nanoparticles have wide-ranging applications across biology, physics, and chemistry. Owing to their biocompatibility, iron nanoparticles produced via green methods have been employed in disease diagnostics, including bone inflammation, skin infections, tuberculosis, tumors, atherosclerosis, cardiovascular and pulmonary diseases, as well as the detection of hepatitis antibodies [16], and have shown potential in targeted drug delivery systems. Iron nanoparticles selectively target diseased cells by generating reactive oxygen species (ROS) or by modulating specific genes involved in disease progression, without affecting healthy cells. They have also demonstrated potential in antimicrobial, anticancer, and antifungal applications [17]. Iron nanoparticles exert antimicrobial effects by generating reactive oxygen species (ROS), disrupting microbial membrane integrity, and altering the chemistry of cellular macromolecules, ultimately leading to pathogen death. Green-synthesized nanoparticles also exhibit notable photothermal properties, enabling them to absorb heat from visible light, which can be utilized for early-stage sensing, disease management, and therapeutic applications. The photothermal potential of iron

nanoparticles has been previously demonstrated, highlighting their promising role in biomedical applications [18].

Overall, this review comprehensively highlights the plant-mediated green synthesis of iron oxide nanoparticles, focusing on the role of phytochemicals in sustainable nanoparticle fabrication. It further summarizes the different types of iron oxides, their structural and physicochemical properties, and their emerging biological applications.

Nanomaterials in the Modern World

Material with any internal or external structures on the nanoscale dimension. Nanomaterials are typically organized into three layers—core, shell, and surface—each characterized by distinct functional groups such as metal ions, small molecules, surfactants, and polymers [19]. Typically, the core of nanoparticles can interact with a variety of morphology and macromolecules, including metal-organic frameworks (MOFs), carbon nanotubes, composites and polymer. This versatility contributes to their distinctive characteristics, such as shape, structural architecture, size, and composition which can be tailored and optimized through specific synthesis methods [20]. Various types of nanomaterials have been reported in the literature. Currently, commonly used nanomaterials include polymeric nanoparticle, carbon-based nanostructures, metal based nanoparticles, zeolites and self-assembled monolayers on mesoporous supports (SAMMS), biopolymers, as well as nanoscale metal oxides and chalcogenide-based semiconductor photocatalysts [21].

Metal based nanoparticle

Metal based nanoparticle are nanostructures synthesized from metallic precursors, which can exist in the form of nanosized metals, metal oxide, metal sulfides, or metal phosphates [22]. There are different types of metal-based nanoparticle that are utilized in various domains. The simplest group includes metallic nanoparticles such as manganese, iron, silver, and gold, which are widely investigated for their roles in therapeutics, bioimaging, electronic devices, and as antimicrobial and magnetic agents. Another important category is doped metal nanoparticles, where elements like palladium, selenium, or zinc are incorporated into host system (e.g., Ag-CuO, Pt-ZnO). These doped systems enhance reactivity, stability, and selectivity, making them useful in cancer therapy, biosensing, catalysis, and biomedical imaging. Sulfide-based metal nanoparticles, including FeS, CuS, And ZnS, have also attracted attention for their antimicrobial effects, drug delivery capabilities, and potential in photothermal therapy. A more extensively studied group is metal oxide nanoparticles, such as CeO_2, ZnO, CuO, and similar oxides, which find applications in drug delivery, bioimaging, antibacterial coatings, photocatalysis, and electronic devices. In addition, metal -organic framework (MOF) nanoparticles like Zr-MOF and Mn-MOF are gaining prominence due to their highly porous structures and tunable properties, enabling applications in targeted drug delivery, biosensing, and therapeutic diagnostics. Metal-based nanoparticles (MNPs) have found applications across various fields owing to their distinctive properties. Properties including shape, size, composition, and surface chemistry play a key role in influencing their toxicity. At the nanoscale, these materials display unique physicochemical behaviors, which make them highly useful in areas including catalysis, electronics, biological systems, and biomedical applications [23]. Metal-based nanoparticles (MNPs) are extensively employed as carriers for drugs, biomolecules, and genes in medical therapies. They are also utilized in imaging and for active or passive targeting of tumor cells, functioning as both carriers and contrast agents. The advancement of these nanoparticles has paved the way for innovative drug delivery systems, precise site-specific targeting, and efficient gene delivery [24].

Iron-based nanoparticles have attracted significant interest among metal-based nanoparticles owing to their notable properties, including structural stability, low toxicity, and pronounced magnetic characteristics, which arise from their high surface area and conductivity. Additionally, their relatively low cost and status as the second most abundant metal on Earth contribute to their widespread use [25].

Iron Based Nanoparticles

Iron based nanoparticles are nanostructured materials composed of iron or its compounds (such as oxides, hydroxides, or doped forms) with sizes typically below 100 nm.

ISSN No. 2454-6194 | DOI: 10.51584/IJRIAS |Volume XI Issue VI June 2026

Varieties of Iron-Based Nanoparticles in Modern Research

Although nanostructures of iron can be classified into several forms, iron oxide nanoparticles stand out as the most important categories due to their broad utility. An overview of the major forms of iron oxide nanoparticles is presented below.

Iron oxide nanoparticles

Iron readily reacts with oxygen in the presence of moisture, resulting in the fabrication of iron oxides. These oxides are commonly found in nature, occurring in soils, rocks, rivers, lakes, ocean floors, and even within living organisms [26]. Iron oxides collectively refer to oxides, oxyhydroxides, and hydroxide composed of Fe(II) and/or Fe(III) cations along with O^{2-} and/or OH^- anions. Till date, seventeen crystalline forms of iron oxide have been detected and analyzed. These phases are generally classified into two main categories: hydrated and anhydrous (non-hydrated) iron oxides. Hydrated iron oxides hold water molecules within their crystal structures and include minerals such as goethite (α-FeOOH), akaganeite (β-FeOOH), lepidocrocite (γ-FeOOH), feroxyhyte (δ-FeOOH), ferrihydrite ($5Fe_2O_3 \cdot 9H_2O$), high-pressure FeOOH, schwertmannite ($Fe_8O_8(OH)_6(SO_4)_n \cdot nH_2O$), and green rust or green-rust-like compounds [27]. Hydrated iron oxides have often been employed as starting materials for the preparation of non-hydrated iron oxide forms, as they experience structural phase changes upon thermal treatment, releasing water from their crystal structures. Non-hydrated iron oxides are generally categorized according to the iron oxidation state in their crystalline framework: (i) wüstite (FeO) containing only Fe^{2+} ions; (ii) ferric oxide (Fe_2O_3) containing only Fe^{3+} ions; and (iii) magnetite (Fe_3O_4), containing both Fe^{2+} and Fe^{3+} ions. While wustite and magnetite each have a single crystal structure, iron(III) oxide exhibits considerable polymorphism, means it exists in several crystalline forms while retaining the same chemical composition but they exhibit different physical properties. Apart from the amorphous form, five stable polymorphs of Fe_2O_3 have been identified under ambient conditions: hematite (α-Fe_2O_3), β-Fe_2O_3, maghemite (γ-Fe_2O_3), ε-Fe_2O_3, and the more recently discovered ζ-Fe_2O_3 (Fig. 1) [28]. The most well-known oxide forms of iron is maghemite (γ-Fe_2O_3), magnetite (Fe_3O_4), and hematite (α-Fe_2O_3) [29] have been widely employed as nanoadsorbents for the removal of various contaminants, including Cr(VI), MnO_4, Pb(II), As(V), $Cr_2O_7^{2-}$, Cu(II) and Hg(II) from environmental and industrial wastewater [30].

Ferric oxide (Fe_2O_3)

Ferric oxide, or iron(III) oxide (O=Fe–O–Fe=O), commonly known as rust, appears in red to brown hues. It is formed through the thermal dehydration of $Fe(OH)_3$ and FeO(OH) at temperatures exceeding 200 °C.", as illustrated in Equations (1) and (2), and can exist in both hydrated and anhydrous forms:

$$2Fe(OH)_3 \rightarrow Fe_2O_3 + 3H_2O \quad (1)$$

$$2FeO(OH) \rightarrow Fe_2O_3 + H_2O \quad (2)$$

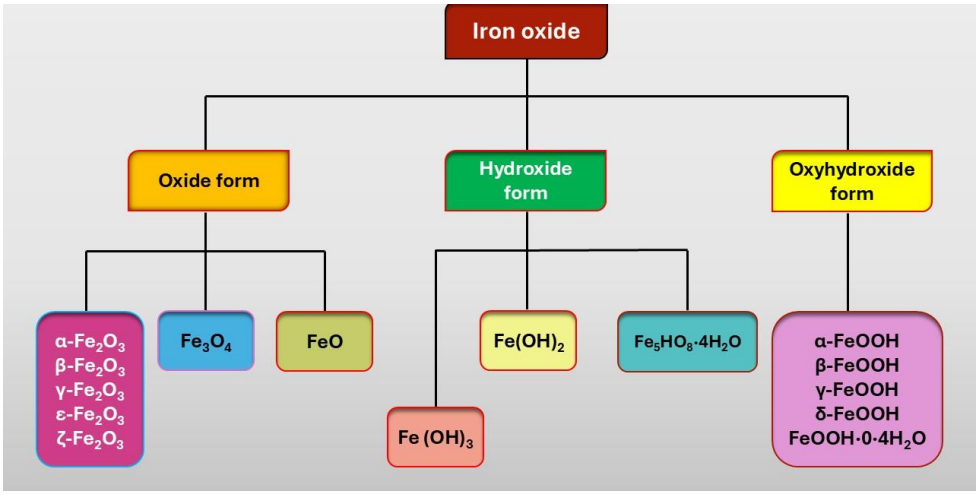

Fig. 1. Different forms of iron-based nanoparticles

ISSN No. 2454-6194 | DOI: 10.51584/IJRIAS |Volume XI Issue VI June 2026

Anhydrous ferric oxides

Anhydrous ferric oxide exists in several polymorphic forms, including alpha (α-Fe_2O_3), beta (β-Fe_2O_3), gamma (γ-Fe_2O_3), and epsilon (ε-Fe_2O_3) as shown in (Fig. 2) These minerals possess identical chemical structure but vary in their crystal system [31].

Hematite (α-Fe_2O_3)

The term hematite (α-Fe_2O) is derived from the Greek word *hematicos*, meaning "blood-red." The formation of hematite from the magnetite is depicted in Equation (3).

$$2Fe_3O_4+1/2O_2 \rightarrow 3(\alpha\text{-}Fe_2O_3) \quad (3)$$

Hematite (α-Fe_2O_3) is naturally occurs in soils and rocks, particularly in sedimentary rocks where it occurs as a precipitates or detrital particles. It is recognized as the earliest known iron ore to have formed on Earth [32]. α-Fe_2O_3 (hematite) adopts a corundum-type crystal structure, (similar to ilmenite ($FeTiO_3$) and corundum) with an R-3c space group and lattice parameters of a = 5.034 Å and c = 13.752 Å. It exhibits both rhombohedral and hexagonal crystal systems, and its crystal habit can take the form of bar, square, spherical, spindel, and oval shapes. Finely powdered hematite appears reddish, whereas bulk samples are typically black or gray. α-Fe_2O_3 undergoes two magnetic transitions: the Néel temperature at approximately 950 K and the Morin transition around 265 K, driven by the interplay between strong magnetic dipolar anisotropy and local ion anisotropy with distinct thermal dependencies. The magnetic behavior is closely related to nanoparticle size and morphology, with smaller particles often displaying superparamagnetic properties above the blocking temperature [26]. As an n-type semiconductor, hematite has a broad band gap of about 2.1 eV, the largest among iron(III) oxide polymorphs, but exhibits very low hole mobility [33]. This mineral is considered valuable, with finely cut black crystals used in jewelry, while its powdered form is employed as a red pigment [34] and in anti-rust applications [26]. α-Fe_2O_3 thin films have facilitated the use of iron(III) oxide polymorphs not only in the production of electrodes for water photoelectrolysis to generate hydrogen but also as a promising material for gas and humidity sensors and lithium-ion battery electrodes [33, 35]. Hematite nanoparticles demonstrate a strong capacity for removing metal ions from aqueous solutions and can be effectively used to treat acid mine drainage. These nanoparticles have been shown to completely remove Mn, Al, Mg and Fe ions, while eliminating over 80% of Zn and Ni ions and up to 72% of Na and Ca ions [36].

β-Fe_2O_3 constitutes a rare crystalline form of iron(III) oxide that was first identified in 1956. This polymorph represents a metastable phase with a bixbyite-type structure belonging to the Ia-3 space group and a lattice parameter of a = 9.393 Å. Under ambient conditions it is paramagnetic in nature, becomes magnetically ordered at 110 K, and exhibits antiferromagnetic behavior at below 110K. Recently, β-Fe_2O_3 has been identified as a promising phase for photo-assisted water splitting. Owing to its narrower band gap compared to hematite, it demonstrates enhanced light absorption and superior performance in photoelectrochemical processes [37]. The β-Fe_2O_3 phase with an approximate band gap of 1.9 eV, prepared as a thin film has been effectively employed for photo-assisted hydrogen generation as an alternative iron oxide photocatalysts [38].

Maghemite (γ-Fe_2O_3)

Maghemite, recognized in 1925, is known to be the second most prevalent polymorphic form of ferric oxide. Maghemite is commonly found in a range of soils, with a notable presence in intensely weathered and contaminated soils of tropical and subtropical regions. Recent studies employing environmental magnetic techniques have further demonstrated its global distribution, with occurrences reported in tropical, subtropical, arid, and tundra zone [39]. Maghemite exhibits an inverse spinel crystal structure with a lattice parameter of a = 8.351 Å. It can crystallize in both cubic and tetragonal systems, typically forming crystals with cubic, plate-like, or spindle shapes. The mineral generally appears brown to reddish-brown in color [40]. Similar to α-Fe_2O_3 and β-Fe_2O_3, γ-Fe_2O_3 behaves as a semiconductor with a bandgap of approximately 2 eV. It is a robust ferrimagnetic material, featuring two magnetic sublattices (i.e. octahedral and tetrahedral) with the Curie temperature estimated between 780 and 980 K. The overall magnetic moment of stoichiometric γ-Fe_2O_3 is 2.5 μB. When the particle size of γ-Fe_2O_3 nanoparticles decreases to around 30 nm, they exhibit

ISSN No. 2454-6194 | DOI: 10.51584/IJRIAS |Volume XI Issue VI June 2026

superparamagnetic behavior. Maghemite nanoparticles can be employed to functionalize other nanostructures, including carbon nanotubes. Such maghemite- coated carbon nanotubes have been utilized in the development of electrocatalysts for the oxygen evolution reaction (OER). Additionally, they have applications in magnetic recording media, the production of biocompatible magnetic fluids, and electrochromic devices [41]. A major area of interest for maghemite nanoparticles is their use in environmental remediation. These nanoparticles demonstrate high efficiency in the eradication of toxic heavy metals, including lead, cadmium, and uranium [42], as well as hexavalent chromium ions [43], from aqueous systems, owing to their strong surface reactivity and adsorption capabilities. Beyond environmental applications, maghemite nanoparticles have also demonstrated potential in agriculture. When incorporated into fertilizers, they can promote plant growth by enhancing nutrient uptake and improving tolerance to abiotic stresses. Studies have shown that treatment with maghemite nanoparticles can increase chlorophyll content, stimulate leaf development, and boost overall biomass, highlighting their promise as components of eco-friendly fertilizer formulations [44]. In addition to environmental and agricultural uses, maghemite nanoparticles have found acceptance in medical and pharmaceutical applications, with FDA approval supporting their use in these fields [45]. Their nanostructures exhibit high magnetic saturation values (near or equal to magnetite nanoparticles) making them well-suited for biomedical applications such as magnetically guided drug delivery, magnetic labeling and hyperthermia-based therapies [46]. Furthermore, maghemite nanoparticles serve as an advantageous platform for the development of dual-functional nanostructures, including fluorescent magnetic nanoparticles. In one study, rhodamine isothiocyanate (RITC) was covalently incorporated into maghemite nanoparticles to create fluorescent magnetic nanostructures for cell labeling. These nanoparticles exhibited pH sensitivity, enabling their use as pH sensors for cellular compartments and animal tissues [47].

ε-Fe_2O_3, a rare and partially stable crystalline form of Fe(III) oxide, was first discovered in 1934 and subsequently reported in detail in 1963. Structurally, this phase crystallizes in an orthorhombic system with a $Pna2_1$ space group [48] and undergoes transformation into hematite (α-Fe_2O_3) when heated between 500 ^{0}C and 750 °C. It exhibits complex magnetic behavior, with notable changes occurring at approximately 490 K (Curie temperature) and 110 K. At RT, ε-Fe_2O_3 exhibits collinear ferrimagnetic behavior, displaying a high coercivity of around 2 T and overall magnetic moment of 1.3 μB [49]. At around 110 K, ε-Fe_2O_3 undergoes another magnetic transition, characterized by a sharp decrease in coercivity and a notable attenuation in the orbital component of the magnetic moment of Fe^{3+} ions. Interestingly, recent studies have also indicated that this compound was utilized in ceramic coating in ancient China [26]. Owing to its remarkable magnetic attributes, rod-shaped ε-Fe_2O_3 particles exhibiting high coercivity have been employed in mesoscopic ferrite bar magnets, which serve as sensitive probes in magnetic force microscopy [50].

The iron(III) oxide polymorph ζ-Fe_2O_3, representing the newest addition to the Fe_2O_3 family, was uncovered in 2015, through high-resolution synchrotron X-ray diffraction investigations. It was formed from the cubic β-Fe_2O_3 phase under high-pressure conditions exceeding 30 GPa and has been designated as zeta-Fe_2O_3 (ζ-Fe_2O_3). After releasing the pressure, the structure remained intact and stable under ambient conditions [51]. The crystal belongs to the I2/a space group, with lattice parameters of a = 9.683 Å, b = 10.00 Å, and c = 8.949 Å. At RT, ζ-Fe_2O_3 exhibits paramagnetic behavior, transitioning to an antiferromagnetic state near the Néel temperature of approximately 69 K [52].

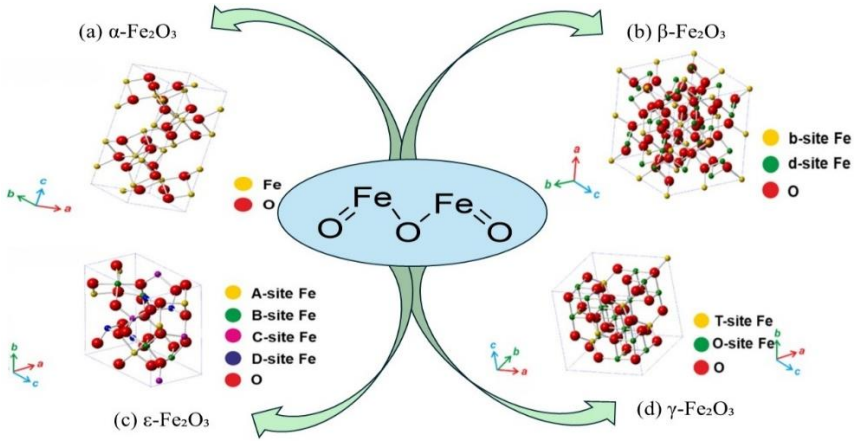

ISSN No. 2454-6194 | DOI: 10.51584/IJRIAS |Volume XI Issue VI June 2026

Figure 2 Crystal structures of non-hydrated iron oxides

Table 1. Overview of Fe_2O_3 polymorphs with their structural and physical attributes.

Polymorphs	Discovery	Crystal St.	Space group	Lattice parameter	Colour
α-Fe_2O_3	-	Corundum type	R-3c	a = 5.034 Å, c = 13.752 Å	When it is finely powdered it exhibits a reddish hue, while in bulk form it appears black or grey.
β-Fe_2O_3	1956	Bixbyite type	Ia-3	a = 9.393 Å	-
γ-Fe_2O_3	1925	Spinel type	-	a = 8.351 Å	Brown or Reddish Brown
ε-Fe_2O_3	1934	-	$Pna2_1$	-	-
ζ-Fe_2O_3	2015	-	I2/a	a = 9.683 Å, b = 10.00 Å, and c = 8.949 Å	-

Hydrous ferric oxide (Ferrihydrite)

The International Mineralogical Association (IMA) officially approved ferrihydrite as a distinct mineral in 1975 [53]. It is a widely studied iron compound, typically represented by the chemical formula $5Fe_2O_3 \cdot 9H_2O$, although alternative compositions including $Fe_2O_3 \cdot 2FeO(OH) \cdot 2.6H_2O$ and $Fe_5HO_8 \cdot 4H_2O$ have also been reported. The chemical formula of ferrihydrite varies due to differences in the amount of water incorporated into its structure. In nature, it is found exclusively as nanocrystals, typically displaying a dark brown to reddish-brown color, and is widely distributed across soils, sediments, hot springs, marine environments, and freshwater systems. Structurally, ferrihydrite crystallizes in a hexagonal close-packed (hcp) system and generally forms spherical crystals. Depending on the arrangement of its constitutive crystallites, ferrihydrite can be classified into two diffraction-based types, known as two-line and six-line ferrihydrite, a distinction derived from the number of scattering bands observed in their X-ray diffraction patterns [54]. Ferrihydrite displays antiferromagnetic behavior, with a weak ferromagnetic-like moment at low temperatures (10 K and 100 K), while remaining paramagnetic at ambient temperature. Furthermore, growth in crystallite size results in a decrease in both magnetization and coercivity [55]. Recent research has focused on injecting colloidal ferrihydrite into the subsurface to form reactive zones that facilitate biodegradation processes. Efforts have also been made to improve the mobility of these nanoparticles within the soil column through polymer coatings as a surface modification approach or by post-flushing with particle-free electrolyte solutions. The application of ferrihydrite nanoparticles not only supports soil microbial activity but also provides benefits to plants. Studies have demonstrated that enriching soil with ferrihydrite nanoparticles can enhance both the development and chlorophyll content of maize seedlings [56]. Ferrihydrite is widely employed for the removal of heavy metals and other ions from aqueous systems. The adsorption of metals such as copper [57], molybdenum [58], lead [59], chromium [60], and zinc [61] primarily occurs through inner-sphere complexation, often resulting in bidentate or bidentate–monodentate complexes, with a specific configuration affected by parameters including pH and metal ion concentration.

Wüstite (FeO)

Iron(II) oxide (ferrous oxide, FeO) was named by the German metallurgist Fritz Wüst (1860–1938). It appears as a gray-black mineral with a slight greenish shade. The chemical formula FeO is not strictly accurate, as wüstite is a naturally non-stoichiometric mineral. In this mineral, the iron content is consistently lower than the stoichiometric ratio, and no temperature exists at which a precise one-to-one ratio between iron and oxygen is observed [62]. At ambient conditions, wüstite (FeO) adopts a highly defective NaCl-type crystal structure, characterized by a nonstoichiometric composition expressed as $Fe_{1-x}O$ [63]. Wüstite is metastable and can

ISSN No. 2454-6194 | DOI: 10.51584/IJRIAS |Volume XI Issue VI June 2026

decompose into a two-phase system consisting of magnetite (Fe_3O_4) and α-Fe. To stabilize wüstite nanoparticles, they are typically coated with organic ligands. Moreover, cubic $Fe_{1-x}O$ can be fabricated under normal pressure for iron deficiencies in the range of $0.05 < x < 0.15$ at 560 °C [64]. Neutron diffraction data indicate that the number of unoccupied octahedral sites is twice of the iron deficiency (x), suggesting that a fraction approximately equal to x of iron atoms occupy interstitial tetrahedral sites. Additional examination of multiple samples shows a direct linear correlation between the stoichiometry of $Fe_{1-x}O$ and its lattice parameter, described by the expression $a\ (Å) = 3.856 + 0.478(1 - x)$ [65]. FeO crystallizes in the $Fm\bar{3}m$ space group with a lattice parameter of a = 4.296 Å. It exhibits antiferromagnetic behavior, with a Néel temperature near 200 K; below this temperature, magnetocrystalline distortion leads to the formation of a rhombohedral crystal structure. From an application perspective, several studies have highlighted the antimicrobial potential of wüstite-based nanostructures. Reports indicate that carbon-coated wüstite nanoparticle chains exhibit strong bactericidal activity, effectively eliminating bacterial cells within a short incubation period even at low concentrations [66]. Wüstite nanoparticles exhibit promising characteristics for use as radiation filters. Glass materials coated with thin layers containing FeO and Fe_2O_3 nanoparticles have been utilized as solar radiation filters. Such coatings can be applied to building windows to reduce heat transmission while still allowing the passage of visible light [67]. Wüstite, possessing a bandgap of approximately 2.1 eV, has been employed as an efficient photocatalyst for the degradation and removal of fluoroquinolone contaminants from aqueous solutions [68].

Ferrous ferric oxide (Fe_3O_4)

Magnetite, chemically known as ferrous ferric oxide, gets its name from the Greek word “magnet,” highlighting its magnetic nature. According to IUPAC nomenclature, it is identified as iron (II, III) oxide, comprising two Fe^{3+} ions and one Fe^{2+} ion combined with four oxygen atoms [26, 31]. Under ambient conditions, they form an inverse spinel cubic structure, classified within the Fd-3m space group [69]. Magnetite appears black with a metallic, opaque sheen and exhibits superparamagnetic behavior at the nanoscale (1–100 nm). At this size range, the nanoparticles cannot retain magnetization once the applied magnetic field is removed. This distinctive property has made Fe_3O_4 nanoparticles widely utilized in various fields, including technology, scientific research, and particularly medical applications [70]. Among the different iron oxides, including FeO, γ-Fe_2O_3, and $FeTiO_3$, Fe_3O_4 is the most widely used due to its high spin polarization at the Fermi level, elevated Curie temperature, notable electrocatalytic activity, structural stability, and straightforward synthesis. Owing to these exceptional physicochemical and magnetic characteristics, Fe_3O_4 nanoparticles have been extensively employed in diverse catalytic and biomedical fields, including cancer therapy, drug delivery, organic synthesis, environmental remediation, biodiesel production, electrocatalysis, and advanced oxidation processes (AOPs) [71].

Iron nanoparticle synthesis method

Various physicochemical and biological approaches have been developed for the fabrication of iron nanoparticles, as illustrated in Figure 3. These synthesis techniques are generally classified into two fundamental strategies: the top-down and bottom-up approaches [72]. In top-down synthesis, bulk materials are broken down into nanosized particles using techniques such as ball milling, etching, laser ablation, sonochemical methods, thermal decomposition, and vacuum sputtering. These approaches generally demand advanced instrumentation and high energy input to convert bulk matter into nanoparticles [73]. Conversely, bottom-up approaches generate nanoparticles from metal precursors through atom-by-atom or molecule-by-molecule assembly, allowing the formation of materials in solid, liquid, or gaseous phases [74]. This approach encompasses various synthesis techniques such as aerosol processes, atomic condensation, precipitation, hydrothermal synthesis, hydrolysis, microemulsion, sol–gel processing, thermal decomposition, and chemical vapor deposition [75]. Despite their effectiveness, these techniques have notable drawbacks. They frequently involve toxic chemicals, produce hazardous by-products, and demand significant energy input. Furthermore, scaling up these processes for industrial production remains challenging, limiting their practical applicability in large-scale manufacturing [76]. To overcome the limitations associated with conventional nanoparticle synthesis, green synthesis approaches have emerged as a sustainable and efficient alternative. These methods are highly cost-effective and can be implemented with relative ease, making them accessible for both laboratory- and industrial-scale applications. Importantly, green synthesis avoids reliance on toxic solvents and

ISSN No. 2454-6194 | DOI: 10.51584/IJRIAS |Volume XI Issue VI June 2026

chemicals, significantly reducing environmental and health risks while minimizing contamination compared to traditional chemical and physical techniques.

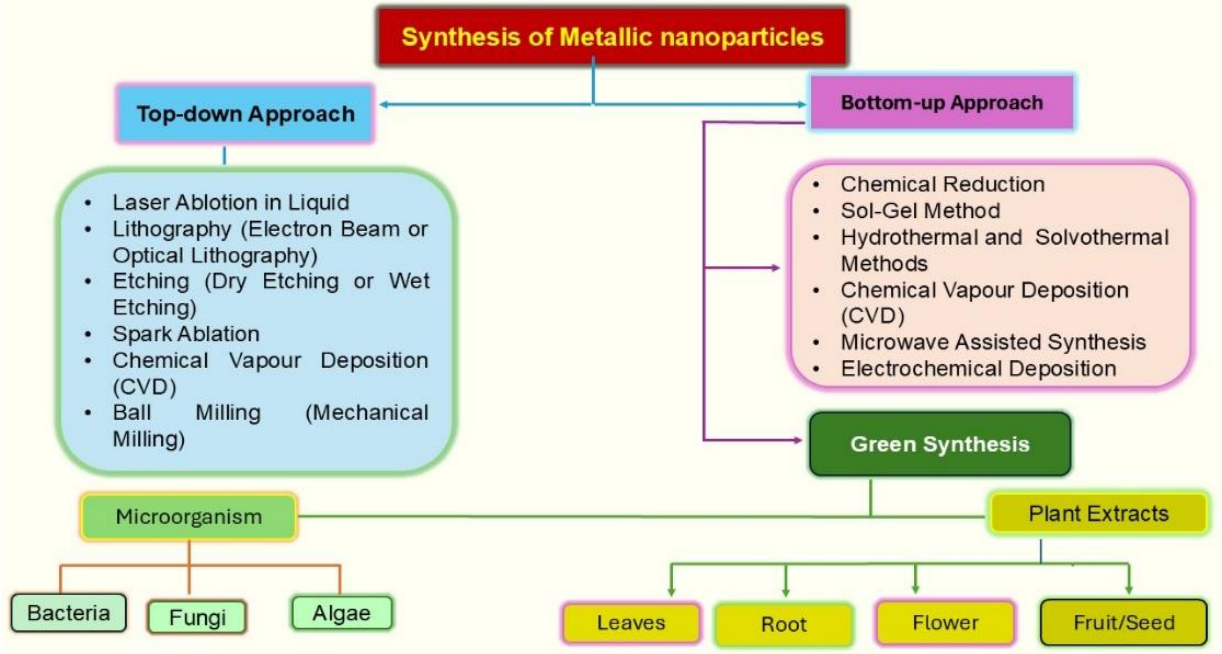

Fig. 3. Different Routes for the Synthesis of Metallic Nanoparticles.

This approach also allows enables fine regulation of nanoparticle morphology and size, enabling the production of well-defined nanostructures tailored for specific applications. Additionally, many green protocols utilize renewable and readily available raw materials, including plant extracts and biological waste, offering opportunities for resource recovery and recycling. The process generally operates under mild conditions without the need for extreme temperatures or high pressures, further enhancing its sustainability. Collectively, these attributes make green synthesis not only environmentally friendly but also highly adapted for large-scale synthesis of nanoparticles, meeting the growing demand for safe and efficient nanomaterials in various fields [77].

Green and Sustainable Fabrication of Iron-Based Nanomaterials

Biological materials, including plants, bacteria, fungi and algae, can be employed in green synthesis to produce iron oxide nanoparticles (IONPs) ranging from 1 to 100 nm in size. These nanoparticles can exhibit a diverse array of shapes, such as cubic, tetragonal, spherical, cylindrical, elliptical, octahedral, orthorhombic, hexagonal rods, nanospheres, and quasi-spherical morphologies. Besides serving as sources for IONP synthesis, these biomaterials can function as capping, reducing, stabilizing, and structuring agents in the green fabrication of NP_S [78].

4.3.1 Eco-Friendly Production of Iron Oxide Nanoparticles Using Plant Extracts: Plants are abundant, simple to cultivate, and also the cost-effective resources that can be employed for synthesizing a variety of nanoparticles [79]. A range of plant parts including leaves, roots, flowers, seeds, peels, fruits, petals, and even whole plants can be employed in the nanoparticle biosynthesis (table 2.). These plant materials are rich in biomolecules consisting of carbohydrates, flavonoids, proteins, amino acid, terpenoids, saponins and nitrogen-containing compounds, which serve as stabilizers, capping agents, reducing agents, and redox mediators during nanoparticle formation [80].

Table 2. Bio fabrication of Iron Oxide Nanoparticles Using Botanical Sources.

Name of the plant and Biomaterial used	Iron precursor used	Size	Shape	Application	Ref.

Tomato **(Fruits)**	$FeCl_3$ (1 M)	48.18–77.54 nm	Semi-spherical	Antibacterial	[81]
Grapes **(Fruits)**	$FeCl_3$ (16.2 g)	49– 50 nm	Cubic	Antibacterial	[82]
Coffee **(Seed)**	Fe^{2+} and Fe^{3+} (1: 1)	23.2– 37.5 nm	Cubic	Antibacterial	[83]
Garlic **(Peels)**	$FeCl_3$ (1 M)	24– 44 nm	Irregular	Degrade methylene blue dye	[84]
Onion **(Peels)**	$FeCl_3$ (1 M)	29– 32 nm	Nanofiber	Degrade methylene blue dye	[84]
Ficus carica **(Leaves)**	$FeCl_3 \cdot 6H_2O$ (0.01 M), NaOH (0.1 M)	43– 57 nm	Agglomerated and are multiform	Multiform antioxidant	[85]
*Camellia sinensisn***(Leaves)**	$FeCl_3$ (10 mM)	13 nm	Cubical	Antioxidant, antimicrobial	[86]
Buddleja lindleyana **(Leaves)**	$Fe(SO_4)_3 \cdot 6H_2O$ (1 g), $AgNO_3$ (0.1 g)	25 and 174 nm	Triangular and spheroidal	Antimicrobial	[87]
Hibiscus rosa sinensis **(Flowers)**	$FeCl_2 \cdot 4H_2O$ (1 mM)	51 nm	Tetragonal	Antibacterial	[88]
Psidium guajava Linn **(Leaves)**	$FeCl_3$ (1 M), NaOH (1 N)	80.3– 99.1 nm	Spherical	Antimicrobial, antioxidant	[89]
Nigella sativa **(Seeds)**	$FeCl_3$ (1 M) and $FeCl_2$ (2 M)	31.45 nm	Spherical	Antimicrobial	[90]
Echinochloa frumentacea **(Grains)**	$Fe(NO_3)$ (0.1 M)	20– 40 nm	Rectangular and triangular	Pharmaceutical, agricultural, targeted drug delivery and biomedical applications	[91]
Iris kashmiriana **(Plant extract)**	-	20– 40 nm	-	Antibacterial, antioxidant	[92]
Momordica charantia **(Fruit)**	-	50– 70 nm	Spherical shaped	removal of heavy metal and microplastic pollutants	[93]
Syzygium aromaticum **(clove)**	ferric nitrate $Fe(NO_3)_3$ $9H_2O$	4.7 nm	-	remove the harmful Cr (VI) ions from an aqueous solution	[94]
Cascabela thevetia	-	47 nm	-	anti-inflammatory, anti-diabetic, and	[95]

(Leaves)				antioxidant properties	
Helianthemum lippii (L.) pers **(Plant extract)**	-	24 to 30 nm.	spheres and irregular forms	antibacterial, antioxidant, and photocatalytic activity	[96]
Cape gooseberry (CG) **(Leaf)**	-	13.9 nm and 15.8 nm	-	antibacterial properties and photocatalytic activity	[97]
Bambusa vulgaris **(Plant extract)**	-	34.6 nm	irregular spherical shape	Enhancing Seed Germination	[98]
Thymus migricus	-	14.74 ± 0.23 nm	-	photocatalytic, antimicrobial, antioxidant, and seed priming properties	[99]
Calotropis procera (Akanal) **(Latex)**	-	between 3 and 5 nm	-	As catalyst for biodiesel production	[100]
Sageretia thea **(dried plant roots)**	-	16.04 nm	-	antibacterial, antifungal Anti-radical potentials (DPPH) and cytotoxicity assays	[101]
Ocimum gratissimum **(Leaves)**	$FeCl_3$ (Merck, India).	5–30 nm	-	act as fertilizer on foliar application	[102]
Anastatica hierochuntica **(Dried plant)**	-	52 nm by XRD and 30–70-nm by SEM	Spherical By SEM	Antibacterial, antioxidant, anti-cancer	[103]

Application

Antibacterial Activities of Fe_3O_4 Nanoparticles

Over the past few years, nanostructured materials have garnered significant interest because various metallic and metal oxide nanomaterials exhibit unique properties and functionalities. Iron oxide nanoparticles (IONPs) possess antibacterial activity similar to free iron ions, unlike the ions, IONPs exhibit minimal toxicity toward human cells. It is proposed that two factors contribute to the antibacterial activity of metal nanoparticles (MNPs): the generation of ROS on the nanoparticle surface regions induces oxidative stress within the bacterial cells, ultimately leading to cell death [104]. Metallic nanoparticles, typically covering a size range of 1–100 nm, represent an emerging area of research with increasing potential applications in the medical field, particularly for combating pathogens, as both Gram-positive and Gram-negative bacteria are responsible for a variety of human diseases [105]. Different synthesized metal oxide nanoparticles have demonstrated inhibitory effects against a range of bacterial strains [106]. $IONP_S$ has the ability to interact with the cellular membranes of bacteria via electrostatic forces, triggering the generation of reactive oxygen species (ROS) that cause oxidative stress and damage within the bacterial cell [107]. Metal ions can interact with protein functional

ISSN No. 2454-6194 | DOI: 10.51584/IJRIAS |Volume XI Issue VI June 2026

groups, such as amino (-NH_2), thiol (-SH) and carboxyl (-COOH) groups, particularly in biocatalysts, resulting in their deactivation or partial inhibition [108]. $IONP_S$ exhibit both magnetic as well as paramagnetic characteristics, and studies have shown that applying an time-varying magnetic field enhances the antibacterial efficacy of Fe_3O_4 nanoparticles against P. mirabilis, A. baumannii and S. epidermidis [109]. Cellular demise and biofilm disruption were induced through photocatalytically generated reactive oxygen species (ROS), while localized heating and mechanical vibrations produced by magnetic fields also contributed to bacterial damage [110]. These conditions lead to bacterial detachment from the biofilm and result in cell wall damage, membrane disruption, cell lysis, and ultimately cell death [111]. Elkhateeb et al. (2024) investigated the antibacterial potential of green-synthesized iron oxide nanoparticles derived from cabbage, turnip, and moringa leaves against *Escherichia coli* (ATCC 25922) and Staphylococcus aureus (PTCC 2592) using the penetration diffusion assay. In their study, a bacterial suspension (10^8 CFU/mL) was prepared and uniformly spread over nutrient agar plates, after which wells were bored into the agar medium. Subsequently, 50 µL of ethanolic iron oxide extract at concentrations of 25, 50, 100, and 200 ppm was added to each well for evaluation of antibacterial efficacy. Following incubation at 37 °C for 24 hours, the diameters of the inhibition zones were recorded. The results revealed that the green-synthesized FeNPs exhibited the greatest antibacterial effect against *E. coli*, with a maximum inhibition zone measuring 8.0 mm [112]. In another related investigation, iron oxide nanoparticles were synthesized using the extract of Iris kashmiriana through a cost-effective and simple conventional heating approach. The antibacterial efficacy of the synthesized iron oxide nanoparticles was evaluated using the disc diffusion method against three Gram-negative bacteria (Escherichia coli, Pseudomonas, and Klebsiella) and one Gram-positive strain (Streptococcus). To assess their antimicrobial efficiency and comparative potential, the nanoparticles were tested in conjunction with the standard antibiotic vancomycin. All the tested Gram-negative and Gram-positive bacterial strains exhibited distinct inhibition zones in response to vancomycin treatment. Furthermore, the synthesized iron oxide nanoparticles demonstrated inhibitory activity against all four bacterial strains, with inhibition zones of 11 mm for Streptococcus pneumoniae, 5 mm for Pseudomonas aeruginosa, 9.5 mm for E. coli, and 10 mm for Klebsiella pneumoniae [92]. The mechanism by which iron oxide nanoparticles inhibit bacterial growth is presented in Figure 4.

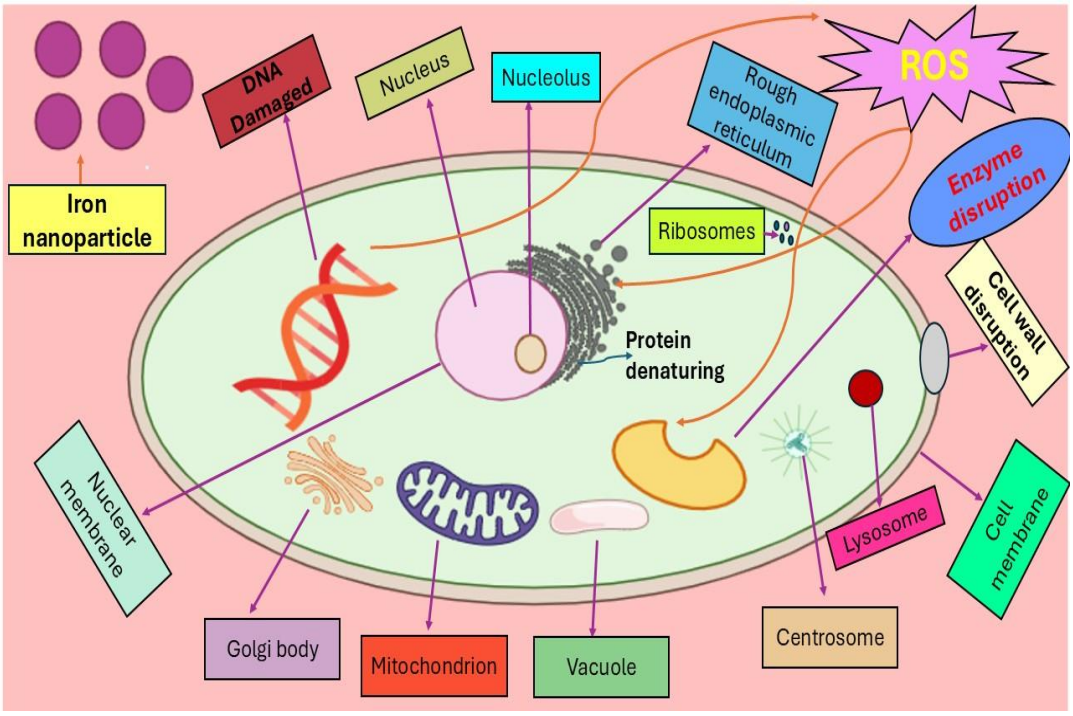

Fig. 4. Proposed mechanism of antibacterial action of iron oxide nanoparticles involving oxidative stress, protein denaturation, and membrane damage.

Anticancer Activity

ISSN No. 2454-6194 | DOI: 10.51584/IJRIAS |Volume XI Issue VI June 2026

Following cardiovascular diseases, cancer is recognized as the second most significant contributor to global mortality. Despite significant advances in medical research, an effective and universally applicable cure for cancer remains elusive, and efforts to discover novel anticancer agents continue worldwide [113].

In this pursuit, Nanotechnology has gained recognition as a potential frontier in disease management. Among various nanoparticles, iron-based nanomaterials have attracted particular interest due to their potential employments in cancer diagnosis, therapy, and drug formulation. Their therapeutic potential is largely associated with their high stability, excellent biocompatibility, and remarkable selectivity toward different cancer cell types [114]. Furthermore, exploiting their magnetic hyperthermia properties provides an additional strategy to selectively induce cancer cell death without damaging surrounding healthy tissues [115]. Over the years, iron oxide nanoparticles (IONPs) have been explored for the treatment of several cancer types, including breast, glioblastoma, liver (Hepatoma H22), leukemia (HL60), T-lymphoblast (MOLT-4), and prostate cancers [116]. Across all tested treatments, IONPs demonstrated significant cytotoxic activity against the reported cancer cell lines. Microbially synthesized IONPs enhance oxidative stress, disrupt cellular division, and alter the structural integrity of key macromolecules, ultimately triggering apoptosis and resulting in cell death [116, 117]. Moreover, when combined with conventional anticancer agents, these IONPs further enhanced the overall antitumor efficacy, indicating their synergistic potential in cancer therapy. Considering their promising anticancer effects, these nanoparticles should be investigated in in vivo models to evaluate their therapeutic potential, while carefully monitoring possible toxicity in humans [118]. Nejad et al. (2024) reported the synthesis of iron nanoparticles employing an aqueous extract of *Mentha spicata* as a natural reducing agent. In this procedure, 10 mL of 0.05 M iron (III) chloride hexahydrate ($FeCl_3 \cdot 6H_2O$) solution was combined with 40 mL of the plant extract prepared at a concentration of 100 µg/mL to initiate nanoparticle formation. The resulting mixture was refluxed at 50 °C for one hour, during which a visible color transition from yellow to black confirmed the successful formation of iron nanoparticles. Furthermore, the researchers investigated the biological potential of these materials by examining the effects of *Mentha spicata* extract, unmodified FeNPs, and *Mentha spicata*-functionalized FeNPs on LS174T colon cancer cell lines. The findings revealed that all three treatments exhibited notable cytotoxic activity against LS174T cells, with the *Mentha spicata*-functionalized FeNPs displaying the highest level of anticancer efficacy [119].

Antioxidant activity:

The antioxidant potential of FeNPs produced through biologically mediated synthesis was also assessed. Their nanoscale size, together with polyphenolic compounds in the plant leaf extracts featuring C–O functional groups, contributes to enhanced free radical scavenging and strong antioxidant potential. Antioxidant activity is generally assessed using three standard assay techniques. Among these, the 2,2-diphenyl-1-picrylhydrazyl (DPPH) assay is widely used to assess the free radical scavenging capacity of Fe_2O_3 nanoparticles by measuring their ability to donate hydrogen atoms. The anti-radical activity of the nanoparticles is typically expressed in terms of the percentage of inhibition and the IC_{50} value (mg/mL). This activity is attributed to the interaction between the nanoparticles and DPPH radicals, which leads to electron transfer at the radical site. Similarly, total antioxidant capacity (TAC) is measured in a comparable manner, where hydrogen atoms and electrons from the antioxidant sample are transferred to an oxidizing complex (PPM), indicating the overall antioxidant potential of the material. The effectiveness of this process is affected by variables including the extract's pH, its redox potential, and also by its structural characteristics of the compounds involved. The Oxygen Radical Absorbance Capacity (ORAC) assay evaluates antioxidant activity by comparing sample against a standard oxidant like Trolox, with the results reflecting the presence of bioactive compounds possessing significant antioxidant potential [120-122]. When evaluated for antioxidant activity, Achyranthes aspera exhibited free radical scavenging potential, which was found to be lower than that of ascorbic acid [123]. In contrast, nanoparticles synthesized through the use of Ficus carica demonstrated antioxidant activity where 1 gram of the NPs was equivalent in free radical scavenging to the 5.14 milligram (mg) of ascorbic acid, with the scavenging efficiency improving at the higher concentrations [121]. Phoenix dactylifera L. is rich in polyphenols, exhibiting a total antioxidant capacity of around 180 mg/g [122]. Mirza et al. (2019) reported that, within the identical process conditions, Prunus persica–Fe nanoparticles exhibited greater free radical scavenging activity compared to Agrewia optiva–Fe nanoparticles, despite similarities in size and other properties [120]. The Fe_3O_4 nanoparticles synthesized through an eco-friendly approach using *Cascabela*

ISSN No. 2454-6194 | DOI: 10.51584/IJRIAS |Volume XI Issue VI June 2026

thevetia extract possess significant potential for diverse biomedical applications. The antioxidant potential of the sample was evaluated by monitoring the decline in absorbance at 630 nm, which indicates the scavenging of DPPH radicals due to the hydrogen-donating ability of antioxidant compounds. The observed decline in DPPH absorbance, resulting from the action of antioxidant compounds, reflects their hydrogen-donating capacity and confirms their role in neutralizing free radicals. Among the tested samples, Fe_3O_4 nanoparticles showed the highest antioxidant activity at a concentration of 800 mg/mL, reaching approximately 96.8%, 78.7%, and 35.1%, which was markedly greater than that of the control and the plant extract. Consequently, an evident increase in antioxidant activity was observed with rising Fe_3O_4 nanoparticle concentration, indicating a concentration-dependent enhancement in radical scavenging efficiency [95].

CONCLUSION

Iron-based nanoparticles (FeNPs) are important nanomaterials because of their unique physicochemical, magnetic, and catalytic properties. Different synthesis methods, particularly green synthesis approaches, provide an eco-friendly and cost-effective route for the preparation of stable and biocompatible nanoparticles with controlled size and morphology. Various forms of iron nanoparticles, including FeO, Fe_2O_3, and Fe_3O_4, have shown remarkable potential in several biomedical and environmental applications. These nanoparticles exhibit significant antibacterial, antioxidant, anticancer activities due to their high surface reactivity and ability to generate reactive oxygen species. Overall, Fe-NPs represent a promising class of nanomaterials with broad applications and considerable future potential in sustainable and advanced technologies.

ACKNOWLEDGEMENT

One of the author Ms Nikita sincerely acknowledge University Grants Commission New Delhi for proving Financial Assistanceship in form of JRF vide reference number 241620069710.

REFERENCES

1. Song W, Ge S. Application of antimicrobial nanoparticles in dentistry. Molecules. 2019 Mar 15;24(6):1033.
2. Sabir S, Arshad M, Chaudhari SK. Zinc oxide nanoparticles for revolutionizing agriculture: synthesis and applications. The scientific world journal. 2014;2014(1):925494.
3. Prabhu S, Poulose EK. Silver nanoparticles: mechanism of antimicrobial action, synthesis, medical applications, and toxicity effects. International nano letters. 2012 Dec;2(1):32.
4. Lee Y, Choi JR, Lee KJ, Stott NE, Kim D. Large-scale synthesis of copper nanoparticles by chemically controlled reduction for applications of inkjet-printed electronics. Nanotechnology. 2008 Oct 15;19(41):415604.
5. Toshima N, Yonezawa T. Bimetallic nanoparticles—novel materials for chemical and physical applications. New Journal of Chemistry. 1998;22(11):1179-201.
6. Reddy LH, Arias JL, Nicolas J, Couvreur P. Magnetic nanoparticles: design and characterization, toxicity and biocompatibility, pharmaceutical and biomedical applications. Chemical reviews. 2012 Nov 14;112(11):5818-78.
7. Yang Y, Liu Y, Song L, Cui X, Zhou J, Jin G, Boccaccini AR, Virtanen S. Iron oxide nanoparticle-based nanocomposites in biomedical application. Trends in biotechnology. 2023 Dec 1;41(12):1471-87.
8. Ijaz I, Gilani E, Nazir A, Bukhari A. Detail review on chemical, physical and green synthesis, classification, characterizations and applications of nanoparticles. Green chemistry letters and reviews. 2020 Jul 2;13(3):223-45.
9. Allouche J. Synthesis of organic and bioorganic nanoparticles: an overview of the preparation methods. Nanomaterials: A Danger or a Promise? A chemical and biological perspective. 2012 Aug 7:27-74.
10. El Shafey AM. Green synthesis of metal and metal oxide nanoparticles from plant leaf extracts and their applications: A review. Green Processing and Synthesis. 2020 Jan 1;9(1):304-39.
11. Sajadi SM, Nasrollahzadeh M, Maham M. Aqueous extract from seeds of Silybum marianum L. as a green material for preparation of the Cu/Fe_3O_4 nanoparticles: a magnetically recoverable and reusable catalyst for the reduction of nitroarenes. Journal of colloid and interface science. 2016 May 1;469:93-8.

12. Demirezen DA, Yıldız YŞ, Yılmaz DD. Amoxicillin degradation using green synthesized iron oxide nanoparticles: Kinetics and mechanism analysis. Environmental Nanotechnology, Monitoring & Management. 2019 May 1;11:100219.
13. Al-Ruqeishi MS, Mohiuddin T, Al-Saadi LK. Green synthesis of iron oxide nanorods from deciduous Omani mango tree leaves for heavy oil viscosity treatment. Arabian Journal of Chemistry. 2019 Dec 1;12(8):4084-90.
14. Mirza AU, Kareem A, Nami SA, Khan MS, Rehman S, Bhat SA, Mohammad A, Nishat N. Biogenic synthesis of iron oxide nanoparticles using Agrewia optiva and Prunus persica phyto species: Characterization, antibacterial and antioxidant activity. Journal of Photochemistry and Photobiology B: Biology. 2018 Aug 1;185:262-74.
15. Tan HL, Lim YC, Ng LY, Lim YP. Plant-mediated synthesis of iron nanoparticles for environmental application: Mini review. Materials Today: Proceedings. 2023 Jan 1;87:64-9.
16. Munir M, Hussain S, Anwar R, Waqas M, Ali J. The role of nanoparticles in the diagnosis and treatment of diseases. Scientific Inquiry and Review. 2020 Sep 22;4(3):14-26.
17. Ahmad R. Peroxynitrite induced cytotoxicity and detection in cardiovascular, neurodegenerative and inflammatory disorders. International Journal of Health Sciences. 2022 Nov;16(6):1.
18. Espinosa A, Di Corato R, Kolosnjaj-Tabi J, Flaud P, Pellegrino T, Wilhelm C. Duality of iron oxide nanoparticles in cancer therapy: amplification of heating efficiency by magnetic hyperthermia and photothermal bimodal treatment. ACS nano. 2016 Feb 23;10(2):2436-46.
19. Sone BT, Diallo A, Fuku XG, Gurib-Fakim A, Maaza M. Biosynthesized CuO nano-platelets: physical properties & enhanced thermal conductivity nanofluidics. Arabian Journal of Chemistry. 2020 Jan 1;13(1):160-70.
20. Geng H, Peng Y, Qu L, Zhang H, Wu M. Structure design and composition engineering of carbon-based nanomaterials for lithium energy storage. Advanced Energy Materials. 2020 Mar;10(10):1903030.
21. Mukhopadhyay R, Bhaduri D, Sarkar B, Rusmin R, Hou D, Khanam R, Sarkar S, Biswas JK, Vithanage M, Bhatnagar A, Ok YS. Clay–polymer nanocomposites: Progress and challenges for use in sustainable water treatment. Journal of hazardous materials. 2020 Feb 5;383:121125.
22. Ishtiaq M, al-Rashida M, Alharthy RD, Hameed A. Ionic liquid–based colloidal nanoparticles: applications in organic synthesis. InMetal nanoparticles for drug delivery and diagnostic applications 2020 Jan 1 (pp. 279-299). Elsevier.
23. Virkutyte J, Varma RS. Green synthesis of metal nanoparticles: biodegradable polymers and enzymes in stabilization and surface functionalization. Chemical Science. 2011;2(5):837-46.
24. Jat SK, Bhattacharya J, Sharma MK. Nanomaterial based gene delivery: a promising method for plant genome engineering. Journal of Materials Chemistry B. 2020;8(19):4165-75.
25. Ali A, Shah T, Ullah R, Zhou P, Guo M, Ovais M, Tan Z, Rui Y. Review on recent progress in magnetic nanoparticles: Synthesis, characterization, and diverse applications. Frontiers in chemistry. 2021 Jul 13;9:629054.
26. Cornell RM, Schwertmann U. The iron oxides: structure, properties, reactions, occurrences and uses. John Wiley & Sons; 2003 Oct 17.
27. Guo H, Barnard AS. Naturally occurring iron oxide nanoparticles: morphology, surface chemistry and environmental stability. Journal of Materials Chemistry A. 2013;1(1):27-42.
28. Tuček J, Machala L, Ono S, Namai A, Yoshikiyo M, Imoto K, Tokoro H, Ohkoshi SI, Zbořil R. Zeta-Fe_2O_3–A new stable polymorph in iron (III) oxide family. Scientific reports. 2015 Oct 15;5(1):15091.
29. Chaturvedi VK, Kushwaha A, Maurya S, Tabassum N, Chaurasia H, Singh MP. Wastewater treatment through nanotechnology: Role and prospects. InRestoration of wetland ecosystem: a trajectory towards a sustainable environment 2019 Jun 30 (pp. 227-247). Singapore: Springer Singapore.
30. Zargoosh K, Abedini H, Abdolmaleki A, Molavian MR. Effective removal of heavy metal ions from industrial wastes using thiosalicylhydrazide-modified magnetic nanoparticles. Industrial & engineering chemistry research. 2013 Oct 23;52(42):14944-54.
31. Campos EA, Pinto DV, Oliveira JI, Mattos ED, Dutra RD. Synthesis, characterization and applications of iron oxide nanoparticles-a short review. Journal of Aerospace Technology and Management. 2015;7:267-76.

32. Roberts AP, Zhao X, Heslop D, Abrajevitch A, Chen YH, Hu P, Jiang Z, Liu Q, Pillans BJ. Hematite (α-Fe_2O_3) quantification in sedimentary magnetism: limitations of existing proxies and ways forward. Geoscience Letters. 2020 Jun 15;7(1):8.
33. Shylesh S, Schünemann V, Thiel WR. Magnetically separable nanocatalysts: bridges between homogeneous and heterogeneous catalysis. Angewandte Chemie International Edition. 2010 May 3;49(20):3428-59.
34. Guntlin CP, Ochsenbein ST, Wörle M, Erni R, Kravchyk KV, Kovalenko MV. Popcorn-shaped Fe_xO (Wustite) nanoparticles from a single-source precursor: colloidal synthesis and magnetic properties. Chemistry of Materials. 2018 Feb 27;30(4):1249-56.
35. Wu C, Yin P, Zhu X, OuYang C, Xie Y. Synthesis of hematite (α-Fe_2O_3) nanorods: diameter-size and shape effects on their applications in magnetism, lithium ion battery, and gas sensors. The Journal of Physical Chemistry B. 2006 Sep 14;110(36):17806-12.
36. Asoufi HM, Al-Antary TM, Awwad AM. Green route for synthesis hematite (α-Fe_2O_3) nanoparticles: Toxicity effect on the green peach aphid, Myzus persicae (Sulzer). Environmental Nanotechnology, Monitoring & Management. 2018 May 1;9:107-11.
37. Zhang N, Guo Y, Wang X, Zhang S, Li Z, Zou Z. A beta-Fe_2O_3 nanoparticle-assembled film for photoelectrochemical water splitting. Dalton Transactions. 2017;46(32):10673-7.
38. Carraro G, Maccato C, Gasparotto A, Montini T, Turner S, Lebedev OI, Gombac V, Adami G, Van Tendeloo G, Barreca D, Fornasiero P. Enhanced hydrogen production by photoreforming of renewable oxygenates through nanostructured Fe_2O_3 polymorphs. Advanced Functional Materials. 2014 Jan;24(3):372-8.
39. Chen YH. Thermal properties of nanocrystalline goethite, magnetite, and maghemite. Journal of Alloys and Compounds. 2013 Mar 15;553:194-8.
40. Nurdin I, Johan MR, Yaacob II, Ang BC, Andriyana A. Synthesis, characterisation and stability of superparamagnetic maghemite nanoparticle suspension. Materials Research Innovations. 2014 Dec 8;18(sup6):S6-200.
41. Martinez AI, Garcia-Lobato MA, Perry DL. Study of the properties of iron oxide nanostructures. Research in nanotechnology developments. 2009;19:184-93.
42. Mazarío E, Helal AS, Stemper J, Mayoral A, Decorse P, Chevillot-Biraud A, Novak S, Perruchot C, Lion C, Losno R, Le Gall T. Maghemite nanoparticles bearing di (amidoxime) groups for the extraction of uranium from wastewaters. AIP advances. 2017 May 1;7(5).
43. Jiang W, Pelaez M, Dionysiou DD, Entezari MH, Tsoutsou D, O'Shea K. Chromium (VI) removal by maghemite nanoparticles. Chemical Engineering Journal. 2013 Apr 15;222:527-33.
44. Palmqvist NM, Seisenbaeva GA, Svedlindh P, Kessler VG. Maghemite nanoparticles acts as nanozymes, improving growth and abiotic stress tolerance in Brassica napus. Nanoscale research letters. 2017 Dec;12(1):631.
45. Mercante LA, Melo WW, Granada M, Troiani HE, Macedo WA, Ardison JD, Vaz MG, Novak MA. Magnetic properties of nanoscale crystalline maghemite obtained by a new synthetic route. Journal of Magnetism and Magnetic Materials. 2012 Sep 1;324(19):3029-33.
46. Kumar N, Kulkarni K, Behera L, Verma V. Preparation and characterization of maghemite nanoparticles from mild steel for magnetically guided drug therapy. Journal of Materials Science: Materials in Medicine. 2017 Aug;28(8):116.
47. Perlstein B, Lublin-Tennenbaum T, Marom I, Margel S. Synthesis and characterization of functionalized magnetic maghemite nanoparticles with fluorescent probe capabilities for biological applications. Journal of Biomedical Materials Research Part B: Applied Biomaterials: An Official Journal of The Society for Biomaterials, The Japanese Society for Biomaterials, and The Australian Society for Biomaterials and the Korean Society for Biomaterials. 2010 Feb;92(2):353-60.
48. López-Sánchez J, Muñoz-Noval A, Serrano A, Abuín M, de la Figuera J, Marco JF, Pérez L, Carmona N, De La Fuente OR. Growth, structure and magnetism of ε-Fe_2O_3 in nanoparticle form. RSC advances. 2016;6(52):46380-7.
49. Jin J, Ohkoshi SI, Hashimoto K. Giant coercive field of nanometer-sized iron oxide. Advanced Materials. 2004 Jan 5;16(1):48-51.

50. Ohkoshi SI, Namai A, Yamaoka T, Yoshikiyo M, Imoto K, Nasu T, Anan S, Umeta Y, Nakagawa K, Tokoro H. Mesoscopic bar magnet based on ε-Fe_2O_3 hard ferrite. Scientific reports. 2016 Jun 7;6(1):27212.
51. Tuček J, Machala L, Ono S, Namai A, Yoshikiyo M, Imoto K, Tokoro H, Ohkoshi SI, Zbořil R. Zeta-Fe_2O_3–A new stable polymorph in iron (III) oxide family. Scientific reports. 2015 Oct 15;5(1):15091.
52. Arriortua OK, Insausti M, Lezama L, de Muro IG, Garaio E, de la Fuente JM, Fratila RM, Morales MP, Costa R, Eceiza M, Sagartzazu-Aizpurua M. RGD-Functionalized Fe_3O_4 nanoparticles for magnetic hyperthermia. Colloids and Surfaces B: Biointerfaces. 2018 May 1;165:315-24.
53. Childs CW. Ferrihydrite: A review of structure, properties and occurrence in relation to soils. Zeitschrift für Pflanzenernährung und Bodenkunde. 1992;155(5):441-8.
54. Mohapatra M, Anand S. Synthesis and applications of nano-structured iron oxides/hydroxides—A review. International Journal of Engineering Science Technologies. 2010; *2*(8):127–146.
55. Wang X, Zhu M, Koopal LK, Li W, Xu W, Liu F, Zhang J, Liu Q, Feng X, Sparks DL. Effects of crystallite size on the structure and magnetism of ferrihydrite. Environmental Science: Nano. 2016;3(1):190-202.
56. Tosco T, Bosch J, Meckenstock RU, Sethi R. Transport of ferrihydrite nanoparticles in saturated porous media: role of ionic strength and flow rate. Environmental science & technology. 2012 Apr 3;46(7):4008-15.
57. Scheinost AC, Abend S, Pandya KI, Sparks DL. Kinetic controls on Cu and Pb sorption by ferrihydrite. Environmental Science & Technology. 2001 Mar 15;35(6):1090-6.
58. Brinza L, Vu HP, Neamtu M, Benning LG. Experimental and simulation results of the adsorption of Mo and V onto ferrihydrite. Scientific reports. 2019 Feb 4;9(1):1365.
59. Trivedi P, Dyer JA, Sparks DL. Lead sorption onto ferrihydrite. 1. A macroscopic and spectroscopic assessment. Environmental science & technology. 2003 Mar 1;37(5):908-14.
60. Johnston CP, Chrysochoou M. Mechanisms of chromate, selenate, and sulfate adsorption on Al-substituted ferrihydrite: implications for ferrihydrite surface structure and reactivity. Environmental science & technology. 2016 Apr 5;50(7):3589-96.
61. Trivedi P, Dyer JA, Sparks DL, Pandya K. Mechanistic and thermodynamic interpretations of zinc sorption onto ferrihydrite. Journal of colloid and interface science. 2004 Feb 1;270(1):77-85.
62. Redl FX, Black CT, Papaefthymiou GC, Sandstrom RL, Yin M, Zeng H, Murray CB, O'Brien SP. Magnetic, electronic, and structural characterization of nonstoichiometric iron oxides at the nanoscale. Journal of the American Chemical Society. 2004 Nov 10;126(44):14583-99.
63. Mao HK, Shu J, Fei Y, Hu J, Hemley RJ. The wüstite enigma. Physics of the Earth and Planetary Interiors. 1996 Aug 1;96(2-3):135-45.
64. Schrettle F, Kant C, Lunkenheimer P, Mayr F, Deisenhofer J, Loidl A. Wüstite: electric, thermodynamic and optical properties of FeO. The European Physical Journal B. 2012 May;85(5):164.
65. Valezi DF, Carneiro CE, Costa AC, Paesano Jr A, Spadotto JC, Solórzano IG, Londoño OM, Di Mauro EJ. Weak ferromagnetic component in goethite (α-FeOOH) and its relation with microstructural characteristics. Materials Chemistry and Physics. 2020 May 1;246:122851.
66. Situ SF, Samia AC. Highly efficient antibacterial iron oxide@ carbon nanochains from wustite precursor nanoparticles. ACS applied materials & interfaces. 2014 Nov 26;6(22):20154-63.
67. Chavez-Galan J, Almanza R. Solar filters based on iron oxides used as efficient windows for energy savings. Solar Energy. 2007 Jan 1;81(1):13-9.
68. Jojoa-Sierra SD, Herrero-Albillos J, Ormad MP, Serna-Galvis EA, Torres-Palma RA, Mosteo R. Wüstite as a catalyst source for water remediation: Differentiated antimicrobial activity of by-products, action routes of the process, and transformation of fluoroquinolones. Chemical Engineering Journal. 2022 May 1;435:134850.
69. Usman M, Byrne JM, Chaudhary A, Orsetti S, Hanna K, Ruby C, Kappler A, Haderlein SB. Magnetite and green rust: synthesis, properties, and environmental applications of mixed-valent iron minerals. Chemical reviews. 2018 Feb 21;118(7):3251-304.
70. Majidi S, Zeinali Sehrig F, Farkhani SM, Soleymani Goloujeh M, Akbarzadeh A. Current methods for synthesis of magnetic nanoparticles. Artificial cells, nanomedicine, and biotechnology. 2016 Feb 17;44(2):722-34.

71. Munoz M, de Pedro ZM, Casas JA, Rodriguez JJ. Preparation of magnetite-based catalysts and their application in heterogeneous Fenton oxidation–a review. Applied Catalysis B: Environmental. 2015 Oct 1;176:249-65.
72. Boudouh D, Hamana D, Metselaar HS, Achour S, Chetibi L, Akhiani AR. Low-temperature green route synthesis of Fe_3O_4-C nanocomposite using Olive Leaves Extract. Materials Science and Engineering: B. 2021 Sep 1;271:115276.
73. Sharotri N, Sharma D. Approaches for nanomaterial lab scale synthesis and manufacturing. InNanomaterials in Manufacturing Processes 2022 Aug 2 (pp. 163-188). CRC Press.
74. Abid N, Khan AM, Shujait S, Chaudhary K, Ikram M, Imran M, Haider J, Khan M, Khan Q, Maqbool M. Synthesis of nanomaterials using various top-down and bottom-up approaches, influencing factors, advantages, and disadvantages: A review. Advances in colloid and interface science. 2022 Feb 1;300:102597.
75. Tripathy S, Rodrigues J, Shimpi NG. Top-down and Bottom-up Approaches for Synthesis of Nanoparticles. Nanobiomaterials Perspect. Med. Appl. Diagn. Treat. Dis. 2023 Jun 5;145:92-130.
76. Rastogi A, Singh P, Haraz FA, Barhoum A. Biological synthesis of nanoparticles: An environmentally benign approach. InFundamentals of nanoparticles 2018 Jan 1 (pp. 571-604). Elsevier.
77. Nair GM, Sajini T, Mathew B. Advanced green approaches for metal and metal oxide nanoparticles synthesis and their environmental applications. Talanta Open. 2022 Aug 1;5:100080.
78. Priya, Naveen, Kaur K, Sidhu AK. Green synthesis: An eco-friendly route for the synthesis of iron oxide nanoparticles. Frontiers in Nanotechnology. 2021 Jun 15;3:655062.
79. Noruzi M. Biosynthesis of gold nanoparticles using plant extracts. Bioprocess and biosystems engineering. 2015 Jan;38(1):1-4.
80. Mittal AK, Chisti Y, Banerjee UC. Synthesis of metallic nanoparticles using plant extracts. Biotechnology advances. 2013 Mar 1;31(2):346-56.
81. Abid MA, Kadhim DA, Aziz WJ. Iron oxide nanoparticle synthesis using trigonella and tomato extracts and their antibacterial activity. Materials Technology. 2022 Jul 3;37(8):547-54.
82. Aziz WJ, Abid MA, Kadhim DA, Mejbel MK. Synthesis of iron oxide (β-Fe_2O_3) nanoparticles from Iraqi grapes extract and its biomedical application. InIOP Conference Series: Materials Science and Engineering 2020 Jul 1 (Vol. 881, No. 1, p. 012099). IOP Publishing.
83. Teoh YP, Ooi ZX, Leong SS, Ng PT, Liu WW. Green synthesis of iron oxide nanoparticle using coffee seed extract and its antibacterial activity. J. Eng. Sci. 2021;17(2):19-29.
84. Abid MA, Abid DA, Aziz WJ, Rashid TM. Iron oxide nanoparticles synthesized using garlic and onion peel extracts rapidly degrade methylene blue dye. Physica B: Condensed Matter. 2021 Dec 1;622:413277.
85. Ustun E, Onbas SC, Celik SK, Ayvaz MC, Sahin N. Green synthesis of iron oxide nanoparticles by using Ficus carica leaf extract and its antioxidant activity.
86. Haydar MS, Das D, Ghosh S, Mandal P. Implementation of mature tea leaves extract in bioinspired synthesis of iron oxide nanoparticles: preparation, process optimization, characterization, and assessment of therapeutic potential. Chemical Papers. 2022 Jan;76(1):491-514.
87. Al-Zahrani FA, Salem SS, Al-Ghamdi HA, Nhari LM, Lin L, El-Shishtawy RM. Green synthesis and antibacterial activity of Ag/Fe_2O_3 nanocomposite using Buddleja lindleyana extract. Bioengineering. 2022 Sep 8;9(9):452.
88. Buarki F, AbuHassan H, Al Hannan F, Henari FZ. Green synthesis of iron oxide nanoparticles using Hibiscus rosa sinensis flowers and their antibacterial activity. Journal of Nanotechnology. 2022;2022(1):5474645.
89. Dildar N, Ali SN, Sohail T, Lateef M, Khan ST, Bukhari SF, Fazil P. Biosynthesis, characterization, radical scavenging and antimicrobial properties of Psidium guajava Linn coated silver and iron oxide nanoparticles. Egyptian Journal of Chemistry. 2022 Feb 1;65(2):145-52.
90. Al-Karagoly H, Rhyaf A, Naji H, Albukhaty S, AlMalki FA, Alyamani AA, Albaqami J, Aloufi S. Green synthesis, characterization, cytotoxicity, and antimicrobial activity of iron oxide nanoparticles using Nigella sativa seed extract. Green Processing and Synthesis. 2022 Mar 28;11(1):254-65.
91. Velsankar K, Parvathy G, Mohandoss S, Ravi G, Sudhahar S. Echinochloa frumentacea grains extract mediated synthesis and characterization of iron oxide nanoparticles: A greener nano drug for potential biomedical applications. Journal of Drug Delivery Science and Technology. 2022 Oct 1;76:103799.

92. Imtiyaz A, Singh A, Bhardwaj A. Green synthesis of iron oxide nanoparticles from Iris kashmiriana (Mazar-Graveyard) Plant Extract its characterization of biological activities and photocatalytic activity. Journal of Industrial and Engineering Chemistry. 2025 Mar 25;143:538-51.
93. Narwal N, Katyal D, Bathi JR. Green synthesis of iron oxide nanoparticles using Momordica charantia: Kinetics of removal of heavy metal and microplastic pollutants. Regional Studies in Marine Science. 2025 Sep 1;86:104189.
94. Yadav J, Chauhan P, Rawat RK, Pathak SK, Srivastava S. Syzygium aromaticum-mediated green synthesis of iron oxide nanoparticles for efficient heavy metal removal from aqueous solutions. Journal of the Indian Chemical Society. 2024 Aug 1;101(8):101201.
95. Abid A, Naveed M, Aziz T, Shabbir MA, Mubeen H, Khan AA, Alsmari AF. In-vitro and in-vivo assessments of greenly synthesized iron oxide nanoparticles from Cascabela thevetia plant extract for the treatment of ventricular septal defect. South African Journal of Botany. 2025 Feb 1;177:363-76.
96. Fouhma A, Tamma N, Rebiai A, Bouafia A. Comprehensive study on antibacterial, antioxidant, and photocatalytic activity of iron oxide nanoparticles synthesized using Helianthemum lippii (L.) pers. Journal of Sol-Gel Science and Technology. 2025 Aug;115(2):896-916.
97. Birusanti AB, Espenti CS, Surendra TV, Srinivas B, Srinivasulu M, Peddulaiah K, Rao KM, Han SS. Synthesis and characterization of multi-responsive iron oxide nanoparticles: Evaluation of antibacterial properties and photocatalytic activity. Journal of Molecular Liquids. 2025 Jan 1;417:126619.
98. Ahmad S, Ahmad N, Ahmad MA, Ahmad G, Ercisli S, Munir I, Mohamed HI. Eco-friendly synthesis of iron oxide nanoparticles from Bambusa vulgaris extract for enhancing seed germination and physiological parameters in Oryza sativa. Journal of Soil Science and Plant Nutrition. 2024 Dec;24(4):7385-97.
99. Ashrafi-Saiedlou S, Rasouli-Sadaghiani M, Fattahi M. Green synthesis of iron oxide nanoparticles using Thymus migricus for multifunctional applications in antioxidant, antimicrobial, photocatalytic, and seed priming processes. Heliyon. 2025 Mar 1;11(5).
100. Kumar S, Kumari S, Kumari A, Kondal N, Choudhary P, Dhiman V, Sharma R. Green synthesis of iron oxide nanoparticles from Calotropis procera latex: an eco-friendly catalyst for biodiesel production from Calotropis procera seed oil. Clean Technologies and Environmental Policy. 2025 Oct;27(10):5655-67.
101. Israeel M, Iqbal J, Abbasi BA, Ijaz S, Ullah R, Zarshan F, Yaseen T, Khan G, Murtaza G, Ali I, Alarjani KM. Potential biological applications of environment friendly synthesized iron oxide nanoparticles using Sageretia thea root extract. Scientific Reports. 2024 Nov 16;14(1):28310.
102. John KS, Parvathi MS, Krishna AS, Sidharth A, Geetha T. Ocimum gratissimum mediated green synthesised iron oxide nanoparticles as a plausible nanofertilizer for peanut plant (Arachis hypogaea). Discover Applied Sciences. 2024 Oct 10;6(10):542.
103. Vahini M, Rakesh SS, Subashini R, Loganathan S, Prakash DG. In vitro biological assessment of green synthesized iron oxide nanoparticles using Anastatica hierochuntica (Rose of Jericho). Biomass Conversion and Biorefinery. 2024 Aug;14(16):19005-15.
104. Abdal Dayem A, Hossain MK, Lee SB, Kim K, Saha SK, Yang GM, Choi HY, Cho SG. The role of reactive oxygen species (ROS) in the biological activities of metallic nanoparticles. International journal of molecular sciences. 2017 Jan 10;18(1):120.
105. Sánchez-López E, Gomes D, Esteruelas G, Bonilla L, Lopez-Machado AL, Galindo R, Cano A, Espina M, Ettcheto M, Camins A, Silva AM. Metal-based nanoparticles as antimicrobial agents: an overview. Nanomaterials. 2020 Feb 9;10(2):292.
106. Ismail RA, Sulaiman GM, Abdulrahman SA, Marzoog TR. Antibacterial activity of magnetic iron oxide nanoparticles synthesized by laser ablation in liquid. Materials Science and Engineering: C. 2015 Aug 1;53:286-97.
107. Gold K, Slay B, Knackstedt M, Gaharwar AK. Antimicrobial activity of metal and metal-oxide based nanoparticles. Advanced Therapeutics. 2018 Jul;1(3):1700033.
108. Wang L, Hu C, Shao L. The antimicrobial activity of nanoparticles: present situation and prospects for the future. International journal of nanomedicine. 2017 Feb 14:1227-49.
109. Abdulsada FM, Hussein NN, Sulaiman GM, Al Ali A, Alhujaily M. Evaluation of the antibacterial properties of iron oxide, polyethylene glycol, and gentamicin conjugated nanoparticles against some multidrug-resistant bacteria. Journal of Functional Biomaterials. 2022 Sep 2;13(3):138.

110. Allafchian A, Hosseini SS. Antibacterial magnetic nanoparticles for therapeutics: a review. IET nanobiotechnology. 2019 Oct;13(8):786-99.
111. Dolezalova E, Lukes P. Membrane damage and active but nonculturable state in liquid cultures of Escherichia coli treated with an atmospheric pressure plasma jet. Bioelectrochemistry. 2015 Jun 1;103:7-14.
112. Nejad FS, Alizade-Harakiyan M, Haghi M, Ebrahimi R, Zangeneh MM, Farajollahi A, Fathi R, Mohammadi R, Miandoab SS, Asl MH, Asgharian P. Investigating the effectiveness of iron nanoparticles synthesized by green synthesis method in chemoradiotherapy of colon cancer. Heliyon. 2024 Apr 15;10(7).
113. Jeevanandam J, Barhoum A, Chan YS, Dufresne A, Danquah MK. Review on nanoparticles and nanostructured materials: history, sources, toxicity and regulations. Beilstein journal of nanotechnology. 2018 Apr 3;9(1):1050-74.
114. Patil RM, Thorat ND, Shete PB, Bedge PA, Gavde S, Joshi MG, Tofail SA, Bohara RA. Comprehensive cytotoxicity studies of superparamagnetic iron oxide nanoparticles. Biochemistry and biophysics reports. 2018 Mar 1;13:63-72.
115. Bose S, Hochella Jr MF, Gorby YA, Kennedy DW, McCready DE, Madden AS, Lower BH. Bioreduction of hematite nanoparticles by the dissimilatory iron reducing bacterium Shewanella oneidensis MR-1. Geochimica et Cosmochimica Acta. 2009 Feb 15;73(4):962-76.
116. Srinath R, Somasundaram ST, Dewangan NK, Moorthy RK, Saravanan K, Ravikumar V. Multifarious pharmacological applications of green routed eco-friendly iron nanoparticles synthesized by Streptomyces Sp.(SRT12). Biological trace element research. 2020 Mar 1;194(1):273-83.
117. Majeed S, Danish M, Ibrahim MN, Sekeri SH, Ansari MT, Nanda A, Ahmad G. Bacteria mediated synthesis of iron oxide nanoparticles and their antibacterial, antioxidant, cytocompatibility properties. Journal of Cluster Science. 2021 Jul 1;32(4):1083-94.
118. Hashmi SS, Shah M, Muhammad W, Ahmad A, Ullah MA, Nadeem M, Abbasi BH. Potentials of phyto-fabricated nanoparticles as ecofriendly agents for photocatalytic degradation of toxic dyes and waste water treatment, risk assessment and probable mechanism. Journal of the Indian Chemical Society. 2021 Apr 1;98(4):100019.
119. Nejad FS, Alizade-Harakiyan M, Haghi M, Ebrahimi R, Zangeneh MM, Farajollahi A, Fathi R, Mohammadi R, Miandoab SS, Asl MH, Asgharian P. Investigating the effectiveness of iron nanoparticles synthesized by green synthesis method in chemoradiotherapy of colon cancer. Heliyon. 2024 Apr 15;10(7).
120. Mirza AU, Kareem A, Nami SA, Khan MS, Rehman S, Bhat SA, Mohammad A, Nishat N. Biogenic synthesis of iron oxide nanoparticles using Agrewia optiva and Prunus persica phyto species: Characterization, antibacterial and antioxidant activity. Journal of Photochemistry and Photobiology B: Biology. 2018 Aug 1;185:262-74.
121. Ustun E, Onbas SC, Celik SK, Ayvaz MC, Sahin N. Green synthesis of iron oxide nanoparticles by using Ficus carica leaf extract and its antioxidant activity.
122. Abdullah JA, Eddine LS, Abderrhmane B, Alonso-González M, Guerrero A, Romero A. Green synthesis and characterization of iron oxide nanoparticles by pheonix dactylifera leaf extract and evaluation of their antioxidant activity. Sustainable Chemistry and Pharmacy. 2020 Sep 1;17:100280.
123. Ahmad W, Singh V, Ahmed S, Nur-e-Alam M. A comprehensive study on antibacterial antioxidant and photocatalytic activity of achyranthes aspera mediated biosynthesized Fe_2O_3 nanoparticles. Results in Engineering. 2022 Jun 1;14:100450.